Article

Chinese Science Bulletin

Solid-State Mechanics

February 2011 Vol.56 No.6: 495–501
doi: 10.1007/s11434-010-4218-9

Fractional stochastic description of hinge motions in single protein molecules

WANG JiZeng

Key Laboratory of Mechanics on Disaster and Environment in Western China, Ministry of Education, College of Civil Engineering and Mechanics, Lanzhou University, Lanzhou 730000, China

Received June 18, 2010; accepted August 22, 2010

In this study, it is demonstrated that the motion of hinges in single protein molecules can be modeled as general fractional Langevin dynamics of harmonically bound particles driven by non-local Gaussian noise with a power-law correlation. This conclusion was justified by comparing the theoretical predictions of the proposed model to the existing molecular dynamics simulations performed on the M6I mutant of phage T4 lysozyme and *E. coli* ribonuclease H_1.

fractional Langevin dynamics, protein hinge motion, Laplace inversion

Citation: Wang J Z. Fractional stochastic description of hinge motions in single protein molecules. Chinese Sci Bull, 2011, 56: 495–501, doi: 10.1007/s11434-010-4218-9

Proteins are not static rigid molecules as observed in X-ray crystallographic structures. Rather, proteins are flexible and constantly perform conformational fluctuations around their equilibrium configurations [1–5]. Recent advances in single-molecule fluorescence spectroscopy have confirmed this because researchers have directly observed motions of proteins over a broad timeframe (10^{-3}–100 s) [6,7]. There are usually four levels of structural organization in proteins and the tertiary structure of proteins often defines their biological functions [4]. Understanding how the conformational dynamics of proteins influences their biological function is an unresolved problem of long-standing interest [1–9].

Computer simulations play an indispensable role in characterizing the structure and dynamic properties of molecules [10–19] because direct experimental observations of single-molecule motions within very small temporal and spatial resolutions are difficult. Arnold and Ornstein [14] studied the hinge-bending motions of T4 lysozyme in an aqueous solution on the basis of molecular dynamics (MD) simulations. In comparison to the crystalline environment, this study observed the conformational re-organization of T4 lysozyme. Philippopoulos and Lim [15] performed 500 ps MD simulations on the backbone motion of Escherichia coli ribonuclease H_1 in solution with the aim to understand the NMR-derived backbone model free parameters and X-ray B-factor values of the free enzyme. Although full-atom MD simulations is a successful technique used to describe conformational fluctuations of biomolecules within certain temporal and spatial scales, the functionally interesting long-time results are difficult to obtain due to the time-consuming simulations required. This limitation usually calls for the development of coarse-grained simulation techniques. The author and coworkers [16–19] have proposed a generalized bead-rod model for the Brownian dynamics simulations of strongly confined macromolecules.

Besides MD simulations on single molecules, analytic solutions are sometimes available with the help of advanced mathematical concepts and tools. On the globular protein molecules with compact domains connected by flexible alpha helices, such as lysozyme, the bending motion of each domain can be treated as a one-dimensional Langevin motion of a rigid body connected by a viscoelastic spring [1]. The driving force in this protein motion is assumed to be the Gaussian-type random function of time with localized

email: jzwang@lzu.edu.cn

autocorrelation as described by McCammon et al. [1]. For this case, analytic solutions can easily be obtained. However, this model is based on the localized random process, which may be inaccurate in many biological systems [4]. An alternative possibility is that the behavior of such a system is dominated by a random force with broad band distribution or, more precisely, with a power-law tail, implying the Langevin motion with a slow non-exponential-decay memory. If the memory kernel has the power-law decay, we refer to such a Langevin equation as a fractional Langevin equation. Kou et al. [20,21] reported a model of this type for the fluctuation of displacement between a donor and an acceptor of electron transfer within a protein complex, where the inertia term in the governing equation is disregarded. Other systems, such as a tagged point on the lipid membrane, may also perform fractional Langevin dynamics within a certain time range [22,23]. In view of the broad applications of the fractional Langevin equations, quite a few analytic solutions have been available for the equations under overdamped conditions [20–22,24,25].

In the present study, we aim to establish a fractional stochastic model for the hinge-bending motion of single protein molecules, where domains or backbone regions in the protein are assumed to be bound by harmonic potentials, and perform fractional Langevin motion driven by non-local random forces with a general power-law correlation rather than the localized correlation as suggested by McCammon et al. [1]. Using the techniques of Laplace transform, Taylor expansions and the wavelet-based Laplace inversion method, analytic solutions are obtained for various moments and correlation functions of the velocity and displacement. Comparison between the theoretical predictions and existing molecular dynamics simulations for the M6I mutant of phage T4 lysozyme and E. coli ribonuclease H_1 shows that the fractional model fits the molecular dynamics simulation data very well.

1 Formulation and computational methodology

A particle immersed in a simple liquid like water will perform Brownian motion due to the frequent collisions with the surrounding liquid molecules. The motion can be modeled by a Langevin equation with random thermal force, $F(t)$, which is a white Gaussian noise with zero mean, $<F(t)>=0$, and localized correlation, $<F(t)F(0)>\propto\delta(t)$. This type of motion has been studied extensively (see Uhlenbeck and Ornstein [26]). On the other hand, when the surrounding medium is no longer a simple liquid, but includes complex internal structures, like the cytoplasm, the corresponding thermal forces can be described as zero-centered noises with non-local correlations [4,20–24,27,28], i.e. $<F(t)>=0$, $<F(t)F(0)>=C(t)$, where $C(t)$ is a slow decay function.

The random thermal force is usually related to the friction coefficient or memory kernel through the fluctuation-dissipation theorem if the fluctuation and the dissipation have the same origin [29–31]. Consider the fractional Langevin dynamics in a harmonic potential as

$$m\ddot{X}+\int_0^t K(t-\tau)\dot{X}(\tau)\mathrm{d}\tau+m\omega^2X = F(t)+H(t),\ X(0)=X_0,\ \dot{X}(0)=V_0, \tag{1}$$

where m is the mass, t the time, $X(t)$ the displacement, $\dot{X}$ the velocity, $\ddot{X}$ the acceleration, $K(t)$ the memory kernel with power law tail, ω the frequency parameter, $H(t)$ the applied external force and $F(t)$ the zero-centered broad-band random force with a correlation function:

$$< F(t)F(\tau) >= C(|\, t-\tau\,|). \tag{2}$$

The second fluctuation-dissipation theorem [25–27] reads $C(t)=k_BTK(t)$ with k_B the Boltzmann constant and T the absolute temperature, which ensures that the system will finally reach the equilibrium state; otherwise, for an external noise, the fluctuation-dissipation relation will not hold and the system will never reach equilibrium.

The fractional Langevin eq. (1) can be extensively used to model and explain various anomalous kinetics that are observed in different experiments including the motions of microspheres in biological cells and polymer networks, and conformational fluctuations within a single protein molecule as reviewed in [27]. Analytical solutions are invaluable due to their broad applications. However, for eq. (1) with a general memory kernel, analytic solutions are usually difficult to obtain due to the existence of singular convolution terms with fractional power law [20–22,24,25, 32].

In the case that the memory kernel in eq. (1) obeys a single power-law

$$K(t)=\frac{\xi}{\Gamma(1-\alpha)t^{\alpha}},\quad 0<\alpha<2, \tag{3}$$

where $\Gamma(\cdot)$ is the Gamma function and ξ the friction coefficient. Applying Laplace transform to eq. (1) yields [33–35]

$$\tilde{X}(s)=X_0s\tilde{G}(s)+V_0\tilde{G}(s)+\frac{1}{m}\tilde{G}(s)[\tilde{F}(s)+\tilde{H}(s)], \tag{4}$$

where $\tilde{G}(s)=1/[s^2+m^{-1}s\tilde{K}(s)+\omega^2]$, $\tilde{K}(s)=\xi s^{\alpha-1}$ and the Laplace transform of a function $f(t)$ is defined as $\tilde{f}(s)$.

Performing an inverse Laplace transform to eq. (4), we obtain the expressions of displacement and velocity as

$$X(t)=X_0\dot{G}(t)+V_0G(t)+\int_0^t\frac{\mathrm{d}\tau}{m}G(t-\tau)[F(\tau)+H(\tau)], \tag{5}$$

$$V(t) = X_0\ddot{G}(t) + V_0\dot{G}(t) + \int_0^t \frac{\mathrm{d}\tau}{m}\dot{G}(t-\tau)[F(\tau)+H(\tau)]. \quad (6)$$

The first order moments of displacement and velocity can be obtained through eqs. (5) and (6) as

$$< X(t) >=< X_0 > \dot{G}(t) + < V_0 > G(t) + \int_0^t \frac{\mathrm{d}\tau}{m} G(t-\tau)H(\tau), \quad (7)$$

$$< V(t) >=< X_0 > \ddot{G}(t) + < V_0 > \dot{G}(t) + \int_0^t \frac{\mathrm{d}\tau}{m}\dot{G}(t-\tau)H(\tau), \quad (8)$$

where we have considered <$F(t)$>=0. Using eq. (2), the second order moments of displacement and velocity can be given by [29–31]

$$\sigma_{XX}(t) =< [X(t)- < X(t) >]^2 > = \frac{k_B T}{m}\left\{2\int_0^t \mathrm{d}\tau G(\tau) - G(t)^2 - \omega^2\left[\int_0^t \mathrm{d}\tau G(\tau)\right]^2\right\} + [\int_0^t \frac{\mathrm{d}\tau}{m^2} G(t-\tau)H(\tau)]^2, \quad (9)$$

$$\sigma_{VV}(t) =< [V(t)- < V(t) >]^2 > = \frac{k_B T}{m}\left[1-\dot{G}(t)^2 - \omega^2 G(t)^2\right] + \left[\int_0^t \frac{\mathrm{d}\tau}{m^2}\dot{G}(t-\tau)H(\tau)\right]^2, \quad (10)$$

$$\sigma_{XV}(t) =< [X(t)- < X(t) >]\cdot[V(t)- < V(t) >] > = \frac{k_B T G(t)}{m}\left[1-\dot{G}(t) - \omega^2\int_0^t \mathrm{d}\tau G(\tau)\right] + \int_0^t \frac{\mathrm{d}\tau}{m^2}\dot{G}(t-\tau)H(\tau)\int_0^t \mathrm{d}\tau G(t-\tau)H(\tau). \quad (11)$$

The transfer function $G(t)$ in eqs. (7)–(11) can be obtained by performing an inverse Laplace transform with respect to $\tilde{G}(s)$. To do so, we adopt an idea based on the Taylor series expansion [36,37]. Let $\eta=s^\alpha/(s^2+\omega^2)$, so that the Laplace transform of $G(t)$ can be rewritten as

$$\tilde{G}(s) = \frac{1}{s^2 + \xi m^{-1} s^\alpha + \omega^2} = \frac{s^{-\alpha}\eta}{1+\xi m^{-1}\eta}. \quad (12)$$

In the case that

$$\mathrm{Re}(s) > \left(\frac{\xi}{m}\right)^{1/(2-\alpha)}, \quad (13)$$

we have

$$|\eta| = \frac{\|s\|^\alpha}{\|s^2+\omega^2\|} \leqslant \|s\|^{\alpha-2} \leqslant |\mathrm{Re}(s)|^{\alpha-2} < \frac{m}{\xi}. \quad (14)$$

Then, the Taylor series expansion of $\tilde{G}(s)$ in terms of η gives

$$\tilde{G}(s) = \frac{s^{-\alpha}\eta}{1+\xi m^{-1})\eta} = \frac{m}{\xi s^\alpha}\sum_{n=0}^{\infty}(-1)^n(\xi m^{-1}\eta)^{n+1} = \sum_{n=0}^{\infty}(-1)^n\frac{\xi^n}{m^n}\frac{s^{n\alpha}}{(s^2+\omega^2)^{n+1}}. \quad (15)$$

Performing a Laplace inversion to eq. (15), we obtain

$$G(t) = \frac{\sin(\omega t)}{\omega} + \sum_{n=1}^{\infty}\frac{(-1)^n\xi^n}{m^n n!}t^{(2-\alpha)n+1}E_{2,2-n\alpha}^{(n)}(-\omega^2 t^2). \quad (16)$$

And similarly we have

$$\dot{G}(t) = \cos(\omega t) + \sum_{n=1}^{\infty}\frac{(-1)^n\xi^n}{m^n n!}t^{(2-\alpha)n}E_{2,2-n\alpha-1}^{(n)}(-\omega^2 t^2), \quad (17)$$

$$\int_0^t G(\tau)\mathrm{d}\tau = \frac{1-\cos(\omega t)}{\omega^2} + \sum_{n=1}^{\infty}\frac{(-1)^n\xi^n}{m^n n!}t^{(2-\alpha)n+2}E_{2,2-n\alpha+1}^{(n)}(-\omega^2 t^2), \quad (18)$$

where we have used the formula [30–32]

$$\boldsymbol{L}^{-1}\{j!\frac{s^{a-b}}{(s^a+\lambda)^{j+1}}\} = t^{aj+b-1}E_{a,b}^{(j)}(-\lambda t^a), \quad \text{for } \mathrm{Re}(s) > |\lambda|^{1/a} \quad (19)$$

and considered that $tE_{2,2}^{(0)}(-\omega^2 t^2) = \omega^{-1}\sin(\omega t)$, in which the generalized Mittag-Leffler function [30–32] $E_{a,b}^{(j)}(z)$ is defined as

$$E_{a,b}^{(j)}(z) = \frac{\mathrm{d}^j}{\mathrm{d}z^j}E_{a,b}(z) = \sum_{l=0}^{\infty}\frac{(l+j)!z^l}{l!\Gamma(al+aj+b)}, \quad j=0,1,2,\ldots. \quad (20)$$

For small t values, eqs. (16)–(18) can be approximated as

$$G(t) \approx \frac{\sin(\omega t)}{\omega(1+\xi m^{-1}t)^\alpha}, \quad (21)$$

$$\dot{G}(t) \approx \frac{\cos(\omega t)}{(1+\xi m^{-1}t)^\alpha}, \quad (22)$$

$$\int_0^t \mathrm{d}\tau G(\tau) \approx \frac{1}{\omega^2} - \frac{\cos(\omega t)}{\omega^2(1+\xi m^{-1}t)^\alpha}. \quad (23)$$

It can be easily verified that eqs. (21)–(23) have good accuracy within a few periods of oscillation in comparison to the corresponding exact expressions in eqs. (16)–(19).

On the other hand, for large time t values, we have

$$G(\infty) = \int_0^\infty \mathrm{d}t\dot{G}(t) = \left[s\tilde{G}(s)\right]_{s=0} = 0, \quad (24)$$

$$\dot{G}(\infty)=\dot{G}(0)+\int_0^\infty \mathrm{d}t\ddot{G}(t)=\left[s^2\tilde{G}(s)-G(0)s\right]_{s=0}=0, \quad (25)$$

$$\int_0^\infty \mathrm{d}tG(t)=\tilde{G}(0)=\frac{1}{\omega^2}. \quad (26)$$

In the case that the external force $H(t)$=0, inserting eqs. (24)–(26) into eqs. (9)–(11) yields

$$\sigma_{XX}(\infty)=\frac{k_BT}{m\omega^2}, \quad (27)$$

$$\sigma_{VV}(\infty)=\frac{k_BT}{m}, \quad (28)$$

$$\sigma_{XV}(\infty)=0. \quad (29)$$

We note that these results have been obtained by Wang and Masoliver [30] and some other researchers through somewhat different methods.

In practical applications, the Mittag-Leffler functions and their high order derivatives are usually difficult to calculate especially when the time is large. Here, we adopt a special method of Laplace inversion suggested by the author and coworkers [38,39] to analytically approximate $G(t),\dot{G}(t)$ and $\int_0^\tau G(\tau)\mathrm{d}\tau$. This wavelet-based approach of Laplace inversion has been justified by successful applications in vibration problems associated with randomness [40,41] and fractional damping [38].

Consider a general transfer function $G(t)$ and its Laplace transform

$$\tilde{G}(s)=\frac{1}{s^2+s\tilde{K}(s)m^{-1}+\omega^2}, \quad (30)$$

where $\tilde{K}(s)$ can be the Laplace transform of an arbitrary or a multi-fractional kernel

$$\tilde{K}(s)=\sum_{j=1}^{N}\xi_j s^{\alpha_j-1}.$$

Let $\tau=\omega t$, $\varsigma=s/\omega$, then we have $G(t)=g(\tau)$ and

$$\tilde{G}(s)=\tilde{g}(\varsigma)=\frac{\omega^{-1}}{\varsigma^2+m^{-1}\omega^{-1}\varsigma\tilde{K}(\omega\varsigma)+1}.$$

The analytical Laplace inversion of eq. (30) is usually difficult to obtain using conventional methods. Here we consider the wavelet-based Laplace inversion formula [38,39], which gives

$$G(t)=\lim_{n\to\infty}\frac{1}{2^{n+1}\pi\omega}\times\sum_{k=-\infty}^{\infty}\frac{\exp[(\beta+k2^{-n}i)\omega t]}{(\beta+k2^{-n}i)^2+(\beta+k2^{-n}i)\tilde{K}[\omega(\beta+k2^{-n}i)]m^{-1}\omega^{-1}+1}, \quad (31)$$

where β is a real constant that insures $\mathrm{e}^{-\beta\omega t}G(t)\in\boldsymbol{L}^2(R)$, and n is an integer indicating that eq. (31) has very good accuracy for $\omega t\in[0,2^n\pi]$. In practical computations, the range of index k for the summation can be determined in terms of the typical frequency ω [38,39] of $G(t)$. For example, the maximum and minimum values of k in eq. (31) can be determined once the frequency bandwidth [$\omega_{\min}$, $\omega_{\max}$] of $G(t)$ has been chosen [38].

In the case that $\tilde{G}(s)=1/(s^2+m^{-1}\xi s^\alpha+\omega^2)$, we have

$$G(t)=\lim_{n\to\infty}\frac{1}{2^{n+1}\pi\omega}\times\sum_{k=-\infty}^{\infty}\frac{\exp[(\beta+k2^{-n}i)\omega t]}{(\beta+k2^{-n}i)^2+\xi m^{-1}\omega^{\alpha-2}(\beta+k2^{-n}i)^\alpha+1}\approx\frac{1}{2^{n+1}\pi\omega}\times\sum_{k=k_{\min}}^{k_{\max}}\frac{\exp[(\beta+k2^{-n}i)\omega t]}{(\beta+k2^{-n}i)^2+\xi m^{-1}\omega^{\alpha-2}(\beta+k2^{-n}i)^\alpha+1}. \quad (32)$$

Eq. (32) does not involve the calculations of complicated generalized Mittag-Leffler functions and associated derivatives [30,31], making this equation more convenient in practical applications than eq. (16).

2 Results and discussion

Many proteins function according to their conformational changes, which can be shear motion of small amplitudes, hinge bending motions of large amplitudes, or combinations of the two [4], among which the hinge-bending motion is produced by a few localized rotations of the hinge that leads to the dramatic changes of the rigid domains as a whole. A classical example to demonstrate that the hinge-bending motion can affect the protein function is found in the periplasmic receptors of the bacterial ABC transporter systems [42,43]. In such systems, the amplitude of hinge-bending motions is usually large so that enough space can be created to enclose the small molecule ligand that is bound to the periplasmic proteins [42,43]. Many proteins deform via domain hinge motions, such as T4 lysozyme, the glutamine binding protein, the periplasmic dipeptide binding protein from *E. coli*, and the lysine/arginine/ornithine binding protein [4,44]. Although a few studies have been performed to characterize protein hinge motions [1,2,4], how such motions influence the biological function of proteins remains largely unknown. The development of new techniques and methods for modeling such motion remains a bottleneck that limits further progress in this area.

Here we consider a protein consisting of two rigid domains as shown in Figure 1. We use the single fractional Langevin equation to model the dynamics of the position of an atom $X(t)$ on one of the domains as

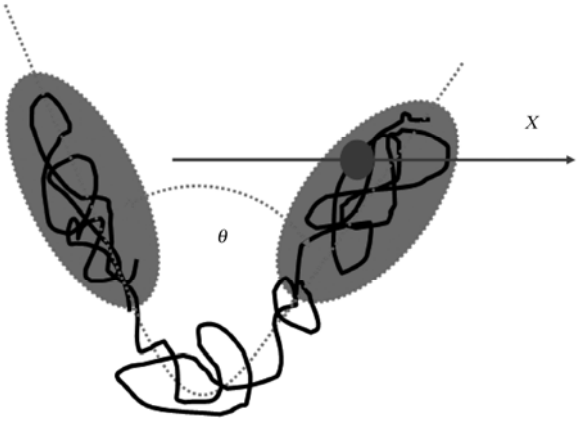

Figure 1 A schematic plot of the hinge-bending motion in a two-domain protein.

$$m\ddot{X} + \xi\int_0^t \mathrm{d}\tau \frac{\dot{X}(\tau)}{\Gamma(1-\alpha)(t-\tau)^{\alpha}} + m\omega^2 X = F(t), \qquad (33)$$

where m represents the mass of the single protein molecule.

The M6I mutant of phage T4 lysozyme with a molecular weight of 18635 Da is composed of two distinct globular domains between which is positioned the active site cleft [1,2,14,45–47]. The molecular structure about M6I is shown in Figure 2, which is taken from the protein data bank (PDB) entry 150L [48]. Arnold and Ornstein [14] using MD simulations studied the hinge bending motion of native and the M6I mutant T4 lysozymes and obtained the root mean square deviation (RMSD) in backbone atom positions. The RMSD values of the M6I trajectory reached a plateau after 275 ps and fluctuate with an amplitude of (2.7±0.1) Å over the final 225 ps of the total 500 ps trajectory. The position of this plateau is at around 2.85 Å. In the Langevin dynamics model, the RMSD reaches $\sqrt{k_B T/(m\omega^2)}$ in the long timeframe limit as shown in eq. (27). Thus we have

$$\sqrt{\frac{k_B T}{m\omega^2}} \approx 0.285 \text{ nm}. \qquad (34)$$

We choose other model parameters in eq. (33) as m=18619 Da, T=300 K. From eq. (34), we can estimate $\omega \approx 40.548$ ns^{-1}. Based on these model parameters, eqs. (16) and (32) provide theoretical predictions on the RMSD values of the M6I trajectory. Figure 2 shows the RMSD obtained based on the model. Eq. (33) can fit the RMSD generated from the MD simulations by Arnold and Ornstein [14] very well when α=0.83 and $\xi/m=3\times10^{11} s^{\alpha-2}$. From Figure 2, we also find that the predictions are sensitive to the values of the parameter α.

To further verify the fractional Langevin model for protein motion, we considered the *E. coli* ribonuclease H_1, which is a potential target for drugs against retroviral diseases, such as HIV infections and AIDS [15,49]. The molecular structure

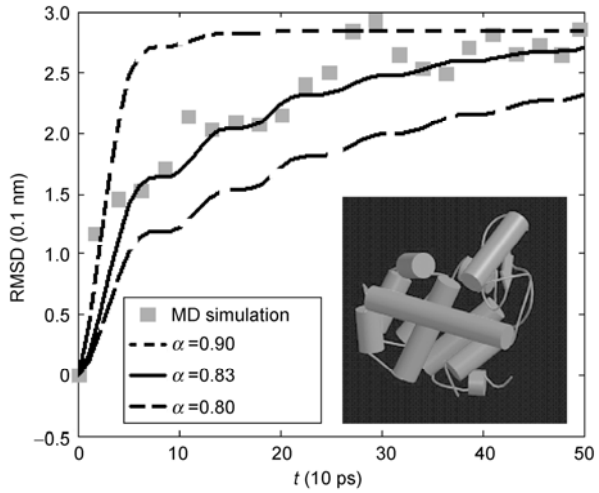

Figure 2 RMSD of the backbone atom positions of the M6I mutant of phage T4 lysozyme. Solid squares represent the MD data by Arnold and Ornstein [14], solid and dashed lines represent the results obtained from eq. (16) using the parameters m=18635 Da, $\xi/m=3\times10^{11} s^{\alpha-2}$, T=300 K, $\omega \approx 40.5$ ns^{-1} and α=0.90, 0.83, 0.80.

(PDB entry 2RN2) is shown in Figure 3 and the protein has a molecular weight of 17581 Da [48,50]. Philippopoulos and Lim [15] using MD simulations studied the backbone motion and obtained the RMSD of the backbone atom positions. The obtained RMSD initially rises but after 100 ps it fluctuates between 1.0 and 1.7 Å. We take the mean position of this plateau as 1.42 Å, which gives $\sqrt{k_B T/(m\omega^2)} = 0.142$ nm. We further take $\xi/m=6.0\times10^{11} s^{\alpha-2}$, T=300 K, then predictions based on the fractional model (33) fit well with the data generated from MD simulations [15] when α=0.83,

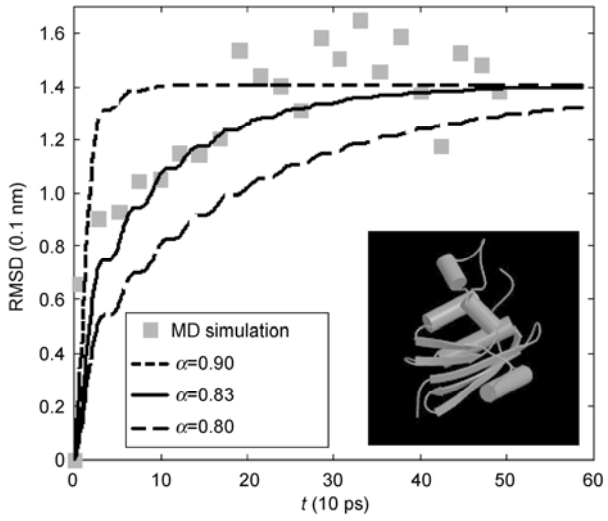

Figure 3 RMSD of the backbone atom positions of *E. coli* ribonuclease H_1. Solid square symbols represent the MD data by Philippopoulos and Lim [15], the solid and dashed lines represent the results obtained from eq. (32) using the parameters m=17581 Da, $\xi/m=6\times10^{11} s^{\alpha-2}$, T=300 K, $\omega \approx 83.9$ ns^{-1} and α=0.90, 0.83, 0.80.

as shown in Figure 3. This observation again confirms that the fractional Langevin model is suitable in describing protein motions. From Figure 3, we also observe that the theoretical predictions sensitively depend on the parameter α, and α=0.83 appears to be a good choice for both cases.

We should note that the theoretical predictions in Figure 3 are obtained using eq. (33) instead of eq. (16). At long times, it is numerically challenging to perform this operation using eq. (16) with the parameter choices for *E. coli* ribonuclease H_1.

3 Conclusions

We have analytically solved the general fractional Langevin equations for harmonically bound particles. For the case of the single fractional memory kernel, solutions based on the Mittag-Leffler functions are obtained using the techniques of Laplace transform and Taylor expansion. The Mittag-Leffler functions and their high-order derivatives are usually difficult to calculate when the time is long. For more general cases of fractional Langevin equations with multi-fractional kernels, we have expressed the solutions using the wavelet-based Laplace inversion technique.

Protein motions are modeled using fractional Langevin dynamics in a harmonic potential. The proposed model can reproduce the RMSDs obtained using MD simulations for the backbone motions of the M6I mutant of phage T4 lysozyme and *E. coli* ribonuclease H_1. Typical model parameter values are justified and provide a reference for future fractional Langevin dynamics modeling of other protein motions. Surprisingly, the parameter α, which characterizes the decay rate of the memory kernel, is found to be ~0.83≈5/6 for two different proteins. Further investigations will focus on determining if 5/6 is a unique decay rate for other proteins.

This work was supported by the National Natural Science Foundation of China (11072094), the Fundamental Research Funds for the Central Universities (lzujbky-2009-13) and the Program for New Century Excellent Talents in Universities, Ministry of Education, China (NCET-10-0445).

1 McCammon J A, Gelin B R, Karplus M. The hinge-bending mode in lysozyme. Nature, 1976, 262: 325–326
2 McCammon J A. Protein dynamics. Rep Prog Phys, 1984, 47: 1–46
3 Yang L W, Bahar I. Coupling between catalytic site and collective dynamics: A requirement for mechanochemical activity of enzymes. Structure, 2005, 13: 893–904
4 Bao G. Mechanics of biomolecules. J Mech Phys Solid, 2002, 50: 2237–2274
5 Blake C C F, Mair G A, North A C T, et al. On the conformation of the hen egg-white lysozyme molecule. Proc R Soc B, 1967, 167: 365–377
6 Yang S, Cao J. Direct measurements of memory effects in single molecule kinetics. J Chem Phys, 2002, 117: 10996–11009
7 Yang H, Luo G, Karnchanaphanurach P, et al. Protein conformational dynamics probed by single-molecule electron transfer. Science, 2003, 302: 262–266
8 Benkovic S J, Hammes-Schiffer S. A perspective on enzyme catalysis. Science, 2003, 301: 1196–1206
9 Daniel R M, Dunn R V, Finney J L, et al. The role of dynamics in enzyme activity. Ann Rev Biophys Biomol Struct, 2003, 32: 69–92
10 Chen W Z, Lu B Z, Wang C X. A simulation method of combinding boundary element method with generalized Langevin dynamics. Chinese Sci Bull, 2000, 45: 2227–2231
11 Wu Z L, Qian S Y, Zheng H J, et al. A drainage-enhancing device for foam fractionation of proteins. Chinese Sci Bull, 2010, 55: 1213–1220
12 Chang S, Gong X Q, Jiao X, et al. Network analysis of protein-protein interaction. Chinese Sci Bull, 2010, 55: 814–822
13 Xia X F, Zhang S, Huang B, et al. Efficient and reproducible folding simulations of the Trp-cage protein with multiscale molecular dynamics. Chinese Sci Bull, 2008, 53: 1699–1707
14 Arnold G E, Ornstein R L. Protein hinge bending as seen in molecular dynamics simulations of native and M61 mutant T4 lysozymes. Biopolymers, 1997, 41: 533–544
15 Philippopoulos M, Lim C. Molecular dynamics simulation of E. coli ribonuclease H1 in solution: Correlation with NMR and X-ray data and insights into biological function. J Mol Biol, 1995, 254: 771–792
16 Wang J, Gao H. A generalized bead-rod model for Brownian dynamics simulations of wormlike chains under strong confinement. J Chem Phys, 2005, 123: 084906–084918
17 Liu B, Wang J, Fan X, et al. An effective bead-spring model for polymer simulation. J Comput Phys, 2008, 227: 2794–2807
18 Wang J, Gao H. Stretching a stiff polymer in a tube. J Mater Sci, 2007, 42: 8838–8843
19 Wang J, Fan X, Gao H. Stretching short DNAs in electrolytes. MCB, 2006, 3: 13–19
20 Kou S C, Xie X S. Generalized Langevin equation with fractional gaussian noise: Subdiffusion within a single protein molecule. Phys Rev Lett, 2004, 93: 180603–180606
21 Min W, Luo G, Cherayil B J, et al. Observation of a power-law memory kernel for fluctuations within a single protein molecule. Phys Rev Lett, 2005, 94: 198302–198305
22 Granek R, Klafter J. Anomalous motion of a membrane segment under an external potential. Europhys Lett, 2001, 56: 15–21
23 Klafter J, Shlesinger M F, Zumofen G. Beyond Brownian motion. Phys Today, 1996, 49: 33–39
24 Lutz W. Fractional Langevin equation. Phys Rev E, 2001, 64: 051106–051109
25 Kupferman R. Fractional kinetics in Kac-Zwanzig heat bath models. J Stat Phys, 2004, 114: 291–326
26 Uhlenbeck G E, Ornstein L S. On the theory of Brownian motion. Phys Rev, 1930, 36: 823–841
27 Metzler R, Klafter J. The restaurant at the end of the random walk: Recent developments in the description of anomalous transport by fractional dynamics. J Phys A, 2004, 37: R161–R208
28 Bao J D, Zhou Y Z. Ballistic diffusion induced by a thermal broadband noise. Phys Rev Lett, 2003, 91: 138104–138107
29 Adelman S A. Fokker-Planck equations for simple non-Markovian systems. J Chem Phys, 1976, 64: 124–130
30 Wang K G, Masoliver J. Linear oscillators driven by Gaussian colored noise: Crossovers and probability distributions. Physica A, 1996, 231: 615–630
31 Porra J M, Wang K G, Masoliver J. Generalized Langevin equations: Anomalous diffusion and probability distributions. Phys Rev E, 1996, 53: 5872–5881
32 Agrawal O P. Stochastic analysis of dynamic systems containing fractional derivatives. J Sound Vib, 2001, 247: 927–938
33 Oldham K B, Spanier J. The Fractional Calculus. New York: Academic Press, 1974
34 Podlubny I. Fractional Differential Equations. San Diego: Academic Press, 1999
35 Carpinteri A, Mainardi F. Fractals and Fractional Calculus in Continuum Mechanics. Wien and New York: Sprigner Verlag, 1997, 291–348
36 Tan W C, Xu M Y. The impulsive motion of flat plate in a generalized second grade fluid. Mech Res Commun, 2002, 29: 3–9

37 Khan M, Nadeem S, Hayat T, et al. Unsteady motions of a generalized second-grade fluid. Math Comput Model, 2005, 41: 629–637
38 Wang J, Zhou Y H, Gao H. Computation of the Laplace inverse transform by application of the wavelet theory. Commun Numer Meth Eng, 2003, 19: 959–975
39 Wang J, Gao H. A simplified formula of Laplace inversion based on wavelet theory. Commun Num Meth Eng, 2005, 21: 527–530
40 Koziol P, Cristinel M, Ibrahim E. Wavelet approach to vibratory analysis of surface due to a load moving in the layer. Int J Solids Struct, 2008, 45: 2140–2159
41 Koziol P, Hryniewicz Z. Analysis of bending waves in beam on viscoelastic random foundation using wavelet technique. Int J Solids Struct, 2006, 43: 6965–6977
42 Magnusson U, Chaudhuri B N, Ko J, et al. Hinge-bending motion of d-Allose-binding protein from Escherichia coli three open conformations. J Biol Chem, 2002, 277: 14077–14084
43 Newcomer M E, Lewis B A, Quiocho F A. The radius of gyration of L-arabinose-binding protein decreases upon binding of ligand. J Biol Chem, 1981, 256: 13218–13222
44 Subbiah S. Protein Motions. Austin, TX: Chapman & Hall, 1996
45 Matthews B W, Remington S J. The three-dimensional structure of the lysozyme from bacteriophage T4. Proc Natl Acad Sci USA, 1974, 71: 4178–4182
46 Matthews B W, Remington S J, Anderson W F. Relation between hen egg white lysozyme and bacteriophage T4 lysozyme: Evolutionary implications. J Mol Biol, 1981, 147: 545–558
47 Faber H R, Mathews B W. A mutant T4 lysozyme displays 5 different crystal conformations. Nature, 1990, 348: 263–266
48 Berman H M, Westbrook J, Feng Z, et al. The protein data bank. Nucleic Acids Res, 2000, 28: 235–242
49 Yang W, Hendrickson W A, Crouch R J, et al. Structure of ribonuclease H phased at 2 Å resolution by MAD analysis of the selenomethionyl protein. Science, 1990, 249: 1398–1405
50 Katayanagi K, Miyagawa M, Matsushima M, et al. Structural details of ribonuclease H from E. coli as refined to an atomic resolution. J Mol Biol, 1992, 223: 1029–1052